

Characterization of a New Rare-Earth-Free Cu-based Bulk Metallic Glass

Tamara D. Koledin,¹ Jaskaran Singh Saini,¹ Donghua Xu,¹ and Melissa K. Santala^{1*}

¹School of Mechanical, Industrial, and Manufacturing Engineering, Oregon State University, Corvallis, OR, United States.

*melissa.santala@oregonstate.edu

Bulk metallic glasses (BMGs) have an amorphous structure containing no crystal defects, which can lead to an increase in hardness, strength, elasticity¹ and corrosion resistance,² relative to their crystalline counterparts. Potential applications of BMGs include coatings, sports utilities (e.g., golf clubs), structural components (e.g., gears and springs) and electronic casing.¹ The main barriers to the widespread use of BMGs are their limited critical casting thickness L_c (reflecting glass-forming ability) and ductility.³ In response, efforts are being made to develop BMGs with improved L_c and ductility. These efforts have included the study of partially and fully crystallized BMGs to understand the mechanisms and kinetics of crystallization that competes against glass formation, which can further help understand the origin of and the limitation to the glass-forming ability.⁴ Recently a rare-earth-free, Cu-based BMG has been developed, $\text{Cu}_{46}\text{Zr}_{33.5}\text{Hf}_{13.5}\text{Al}_7$ (at.%) which has been shown to have an L_c of 28.5 mm, highest among all copper based alloys.⁵ CuZr-based BMGs have been shown, in differential scanning calorimetry (DSC), to have two crystallization peaks.⁶ This is also the case for $\text{Cu}_{46}\text{Zr}_{33.5}\text{Hf}_{13.5}\text{Al}_7$ which has peaks at 475°C at 34 minutes and 65 minutes. In this work, transmission electron microscopy (TEM) characterization was performed on as-cast and thermally annealed $\text{Cu}_{46}\text{Zr}_{33.5}\text{Hf}_{13.5}\text{Al}_7$ to determine the phases associated with the calorimetric data.

$\text{Cu}_{46}\text{Zr}_{33.5}\text{Hf}_{13.5}\text{Al}_7$ specimens made from 10 mm diameter tilt cast rods were characterized as cast and after isothermal annealing at 475°C for 34 and 65 minutes to obtain one partially and one fully crystallized sample respectively. The phases and their chemical compositions were determined with selected area electron diffraction (SAED) and scanning TEM (STEM) electron dispersive x-ray spectroscopy (EDS) using an FEI Titan TEM/STEM operated at 200 keV. The as-cast BMG was amorphous as expected (Fig. 1a). The specimen annealed for 34 min at 475°C, which corresponds to the first DSC peak, was partially crystalline with grains varying from ≈ 100 to 500 nm (Fig. 1b). Based on SAED, this primary phase was found to be consistent with orthorhombic phases of $\text{Cu}_{10}\text{Zr}_7$ and $\text{Cu}_{10}\text{Hf}_7$. Along with EDS, the data suggests there is a single primary phase $\text{Cu}_{10}(\text{Zr,Hf})_7$ with the random substitution of Hf for Zr. After 65 minutes at 475°C, the sample was fully crystallized. The $\text{Cu}_{10}(\text{Zr,Hf})_7$ grains appeared to have slightly increased in size along with the emergence of at least one other secondary phase (Fig 1c,d). A secondary phase has been determined to be tetragonal (Strukturbericht C11_b) $\text{Cu}(\text{Zr,Hf})_2$. The nanoscale grains indicate that the crystal growth from the glass matrix is overall sluggish, consistent with the high glass-forming ability of the alloy. The SAED and EDS results suggest that the co-existing Zr ($r = 1.58 \text{ \AA}$) and Hf ($r = 1.67 \text{ \AA}$) with different atomic radii in the competing crystal phases may have contributed to the enhanced glass-forming ability upon substituting part of Zr in the ternary base alloy $\text{Cu}_{46}\text{Zr}_{47}\text{Al}_7$ with Hf. Further TEM studies on the kinetics of crystallization through in-situ or ex-situ (with more time steps and temperatures) annealing of this and other related compositions will help understand why the glass-forming ability reaches its maximum at 13.5% Hf in the series $\text{Cu}_{46}\text{Zr}_{47-x}\text{Hf}_x\text{Al}_7$.⁵

References:

- [1] M Telford. *Materials Today* **7** (2004), p. 36-43. [https://doi.org/10.1016/S1369-7021\(04\)00124-5](https://doi.org/10.1016/S1369-7021(04)00124-5)
- [2] K Tamilselvam, JS Saini, DH Xu, and D Brabazon. *Journal of Materials Research and Technology* **16** (2022), p. 482-494. <https://doi.org/10.1016/j.jmrt.2021.12.027>
- [3] Q Zhang, W Zhang and A Inoue. *Materials Transactions* **48** (2007), p. 1272-1275. <https://doi.org/10.2320/matertrans.MF200620>
- [4] S Lan, X Wei, J Zhou, and Z Lu, *Applied Physics Letters* **105** (2014), 201906. <https://doi.org/10.1063/1.4901905>
- [5] JS Saini, C Palian and DH Xu, *Applied Physics Letters* **116** (2020) 011901. <https://doi.org/10.1063/1.5131645>
- [6] JS Saini, JP Miska, and DH Xu, *Journal of Alloys and Compounds* **882** (2021), p. 160896. <https://doi.org/10.1016/j.jallcom.2021.160896>

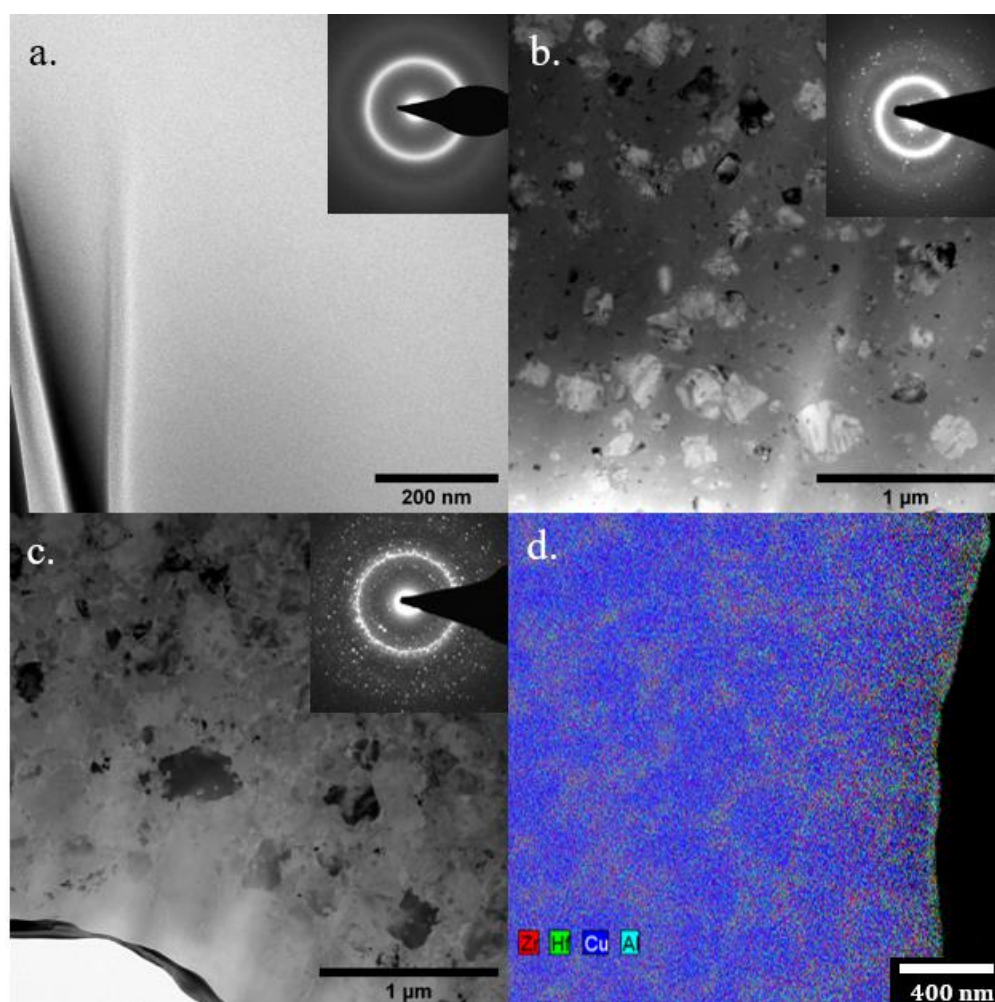


Figure 1. Bright field TEM images with corresponding SAED patterns for (a) amorphous, (b) partially crystallized, and (c) fully crystallized $\text{Cu}_{46}\text{Zr}_{33.5}\text{Hf}_{13.5}\text{Al}_7$. (d) EDS map of a fully crystallized sample showing grains of the Cu-rich primary phase, $\text{Cu}_{10}(\text{Zr},\text{Hf})_7$, surrounded by Zr-rich material which includes $\text{Cu}(\text{Zr},\text{Hf})_2$.